This is a preproof accepted article for *Clay Minerals*
This version may be subject to change during the production process
DOI: 10.1180/clm.2025.10013

Inner and outer surface modification of Algerian halloysite nanotubes with triethoxy(octyl)silane and caffeic acid for enhanced functional properties

Z. A. Mekhania[*1], K. Iggui[2,3], N. Benkacher[1], A. Benhamida[1], N. Bengourna[1] A. Djermoune[4], F. Ait Merzeg[4], H. Satha[1] and A. Layachi[1, 5]

[1] *Laboratoire des Silicates, Polymères et des Nanocomposites (LSPN), Université 8 Mai 1945, 24000 Guelma, Algeria.*

[2] *Département de Technologie Chimique Industrielle, Institut de Technologie, Université de Bouira, 10000 Bouira, Algeria.*

[3] *Laboratoire des Matériaux Polymères Avancés, Faculté de Technologie, Université de Bejaia, 06000 Bejaia, Algeria.*

[4] *Technical Platform for Physico-chemical Analyzes (PTAPC-Bejaia), Scientific and Technical Research Center in Physical and Chemical Analyses (CRAPC), BP384 Bou-Ismail, RP 42004 Tipaza, Algeria.*

[5] *Institut des Sciences et des Techniques Appliquées (ISTA), Université Frères Mentouri Constantine 1, 25000 Constantine, Algeria*.

Running head: *Algerian halloysite surface modification with OTES and Caffeic acid*

DOI :

*Email:mekhaniazeineb@gmail.com;mekhania.zeynebabir@univ-guelma.dz

Abstract:

Halloysite nanotubes (HNT) face significant challenges in their application due to aggregation, poor dispersion, and high hydrophilicity, which limit their integration into polymer matrices. This study introduces a novel functionalisation strategy for Algerian HNT, targeting their inner and outer surfaces with triethoxy(octyl)silane (OTES) for silanisation and caffeic acid (CA) for lumen loading. Comprehensive characterisation techniques were used to analyse pristine and OTES-modified HNT (O-HNT) and CA-loaded HNT (CA-HNT) to evaluate the impact of both selective agents, which successfully altered the structural, textural, chemical, morphological, and thermal HNT properties. The crystalline structure and changes in crystallite size following surface modification were determined using X-ray diffraction (XRD) analysis. BET analysis showed that the surface area of O-HNT increased to 74 $m^2.g^{-1}$ compared to 54 $m^2.g^{-1}$ for HNT, whereas CA-HNT experienced a decrease to 42 $m^2.g^{-1}$ owing to pore obstruction, with a pore size shifting to 10–12 nm for O-HNT and 16 nm for CA-HNT. Fourier-transform infrared spectroscopy (FTIR) and X-ray fluorescence (XRF) confirmed effective surface modification by achieving successful chemical bonding and a shift in the elemental composition. Morphological analysis through Scanning electron microscopy (SEM) revealed considerable morphological changes in both treatments, while Thermogravimetric analysis (TGA) demonstrated that thermal stability of HNT modified with caffeic acid was improved, with a higher decomposition peak at 520°C. These modifications effectively improved the dispersion, thermal stability, and compatibility, offering the modified Algerian HNT potential as a promising green nanofiller in polymer nanocomposite applications, such as active packaging and thermal insulation coatings.

Keywords: Algerian halloysite nanotubes, triethoxyoctylsilane, caffeic acid, selective functionalisation.

https://doi.org/10.1180/clm.2025.10013 Published online by Cambridge University Press

Introduction

Natural nanoclays, have gained significant attention due to their environmentally friendly and cost-effective properties as nanofillers (Nazir *et al.*, 2016; Guo *et al.*, 2018; Elmi, 2023). Halloysite nanotubes (HNT), a subtype of kaolinite, stand out due to their high aspect ratio, abundance, tunable surface chemistry, and porosity (Biddeci *et al.*, 2022a). These unique properties position HNT as an attractive green alternative to synthetic nanomaterials like carbon nanotubes (Liu *et al.*, 2014; Ma *et al.*, 2018; Çankaya *et al.*, 2024), particularly for applications in biomedicine, packaging, and catalysis, as discussed in recent reviews (Kouser *et al.*, 2020; Boccalon *et al.*, 2022; Massaro *et al.*, 2022a; Butun Sengel *et al.*, 2023; Fahimizadeh *et al.*, 2024).

Structurally, HNT formed through the weathering of rocks in tropical and subtropical climates. They typically exhibit a tubular morphology, although they can also appear as spheroids or plates (Wong *et al.*, 2021). These nanotubes follow the chemical formula $Al_2Si_2O_5(OH)_4 \cdot nH_2O$ consisted of a dioctahedral 1:1 two-layered hollow structure made up of aluminosilicate layers rolled together to form their walls, held together by van der Waals forces and hydrogen bonding. The dimensions of HNTs vary, with lengths ranging from 100 nm to 2000 nm and inner diameters of 10–30 nm, while the outer diameters range from 30–50 nm (Joussein *et al.*, 2007; Rawtani *et al.*, 2012; Prishchenko *et al.*, 2018; Ouyang *et al.*, 2019; Kassa *et al.*, 2020).

The surface complexity of HNT includes distinct hydrophilic and hydrophobic regions as reported by Biddeci et al. (2023) and Ganapathy et al. (2022) : a hydrophilic internal lumen with aluminol (Al–OH) groups, a less hydrophilic external surface with siloxane (Si–O–Si) groups, an interlayer surface chemically similar to the internal lumen, and edge surfaces terminated by both aluminol and silanol (Si–OH) groups. This structural complexity contributes to their exceptional thermal stability, mechanical strength, and functional

https://doi.org/10.1180/clm.2025.10013 Published online by Cambridge University Press

properties as explained by Gaaz et al. (2017), making them ideal for reinforcing polymers like polyethylene, epoxy resins, and rubbers (Cheng *et al.*, 2017; Lisuzzo *et al.*, 2020). Even at low concentrations (3–7 wt. %), HNT significantly enhances thermal resistance, mechanical properties, and flame retardancy (Bugatti *et al.*, 2017; Petková *et al.*, 2019), enabling applications in coatings, tissue engineering, and active packaging (Kouser *et al.*, 2022; Qin *et al.*, 2024; Sun *et al.*, 2024; Kim *et al.*, 2025; Zhang *et al.*, 2025a).

In the light of these features, the inherent hydrophilicity of HNT remains a significant challenge, driven by abundant hydroxyl groups on their inner and outer surfaces, along with their strong surface polarity, lead to poor interfacial adhesion and aggregation when integrated into various organic and inorganic matrices (Meng *et al.*, 2017). To overcome these limitations, researchers have explored various surface modification strategies for both outer and inner surfaces of HNT, including acid etching, alkali treatment, polymers, surfactant and nanomaterials. These approaches have proven effective in improving dispersion and compatibility in nanocomposites (Yuan *et al.*, 2015; Tharmavaram *et al.*, 2018; Tarasova *et al.*, 2019).

Previous research has focused primarily on modifying the external surfaces of HNT, exploiting their elongated, nanorod-like shape (Abdullayev *et al.*, 2012; Sargazi *et al.*, 2022), which facilitates interactions through van der Waals forces, hydrogen bonding, electrostatic, and covalent reactions (Kokulnathan *et al.*, 2020; Zhao *et al.*, 2020). These interactions make the surface amenable to functionalisation with various molecules such as : grafting of different metallic nanoparticles (Ni, ZnO, Pt) or functional organic molecules as organophosphonic acid and organosilanes (Sun *et al.*, 2015; Zhang *et al.*, 2016; Jawwad Saif *et al.*, 2018; Taroni *et al.*, 2019; Sadjadi, 2020; Lisuzzo *et al.*, 2023).

Among these, organofunctional alkoxysilanes which have been widely adopted strategy for modifying HNT. It requires the well-understood of silanization chemistry, where

https://doi.org/10.1180/clm.2025.10013 Published online by Cambridge University Press

alkoxysilane hydrolysis forms silanol groups, as they can attach various functional groups to HNT surfaces through covalent bonding. The covalently attached silane molecules form a monolayer or multilayer depending on reaction conditions, thereby functionalizing the HNT surface with desired groups. such as vinyl, epoxy, methacrylate, phenyl, thiol and amine groups, which have been extensively studied for their effectiveness in improving HNT compatibility and functionality with different matrices (Zhang *et al.*, 2016; Yang *et al.*, 2017; Jafazadeh & Haddadi-Asl, 2023; Bao *et al.*, 2024; Senyel & Dike, 2024; Wieczorek *et al.*, 2024).

While surface modifications of the external wall of HNTs are well-documented, strategies targeting the inner lumen, defined by aluminol-rich groups and typically air-filled cavities that serve as a host for guest molecules, remain less explored, primarily due to challenges related to limited access and confined internal spaces. This inner lumen presents a significant challenge for the efficient loading of functional molecules (Biddeci *et al.,* 2016, 2022b; Sahnoune et al., 2017 ; Kaur *et al.,* 2024). Researchers proposed methods such as acid etching to widen the lumen, enabling to encapsulate and release of active agents like drugs, enzymes, dyes, nucleic acids, or nanomaterials. These modifications facilitate applications such as controlled drug release, catalysis, and nanoreactor functionalities, as demonstrated in recent reviews and research papers (Lazzara et al., 2018; Lei et al., 2023; Massaro, Licandro, et al., 2022; Rawtani et al., 2017; Santos et al., 2018; H. Zhang et al., 2017; J. Zhang et al., 2025b).

In this study, distinct modification approaches are explored to prepare organic-inorganic compounds. These approaches involve silanization with triethoxy(octyl)silane (OTES) and caffeic acid (CA) loading, aiming to address the inherent limitations of aggregation and poor dispersibility, particularly in Algerian halloysite nanotubes (HNT), which remain largely underexplored despite their local abundance. This paper also provides a

https://doi.org/10.1180/clm.2025.10013 Published online by Cambridge University Press

comparative evaluation of the effects of these two treatments which have been minimally explored in surface modification studies.

As a chemical agent triethoxy(octyl)silane has proven effective in rendering HNT surfaces by covalently bind to external silanol groups, forming hydrophobic alkyl layers that maintain dispersion in polymer matrices. This medium-length alkyl chain expected to improve compatibility without causing excessive steric hindrance, making it suitable for applications in flexible packaging films, thermally resistant composites, and hydrophobic coatings (Sánchez-Fernández et al., 2014 ; Siy et al., 2020).

However, effective lumen modification requires overcoming the challenge of limited accessibility. To address this, acid etching with weak acids like acetic acid step is applied prior to loading. This treatment selectively removes impurities and increases the lumen diameter for effective loading of guest molecules such as caffeic acid which stands out as a bioactive phenolic compound with strong antioxidant and antimicrobial properties (Katuwavila et al., 2016 ; Maurya & Devasagayam, 2010).

The impact of both treatments on the structural, chemical, textural, and thermal properties of HNT will be assessed using advanced techniques, including Fourier transform infrared spectroscopy (FTIR), X-ray fluorescence (XRF), nitrogen adsorption/desorption isotherms (BET), Scanning electron microscopy (SEM), Thermogravimetric analysis (TGA), and X-ray diffraction (XRD).

The modifications are expected to significantly enhance the dispersion, thermal stability, and compatibility of Algerian HNT, promoting the development of an eco-friendly, high-performance polymer nanocomposites based on HNT making them viable for applications like active packaging, thermal insulation coatings.

https://doi.org/10.1180/clm.2025.10013 Published online by Cambridge University Press

Materials and Methods

Materials

Algerian halloysite nanotubes (HNT), were collected from the Djebel Debbagh deposit in Guelma region, located in northeastern Algeria, distinguished by their greyish colour due to 1.22 wt % MnO_2 content compared to typical halloysite nanotubes. The material was supplied by SOALKA (Société Algérienne des Kaolins), an Algerian kaolin production company. HNT tubes exhibited an average internal diameter range from 10 to 30 nm and an external diameter of 30 to 50 nm, a density of 2.1 $g.cm^{-3}$ and a specific surface area of 54 $m^2. g^{-1}$ (Kennouche *et al.*, 2016)

For prior processing, raw HNT stones were first manually ground into a coarse powder using a hand mortar to facilitate the ball mill processing. The coarse powder was then refined using a laboratory ball mill for 1 hour and sieved through a 38 µm mesh to yield microparticles with an average diameter of 25 µm, containing a fraction of nanoparticles.

For surface modification, caffeic acid (CA) and triethoxy(octyl)silane (OTES) were procured from Sigma Aldrich (France) for surface treatment of HNT. Acetic acid (99.7% CH_3COOH) was employed as a mild acid to enhance the lumen size in HNT.

HNT silanisation

Silane modification followed the procedure outlined by Carli *et al.* (2014). Approximately 20 g of HNT was dispersed in 120 mL of 96% ethanol solution. Triethoxy(octyl)silane was added at 1:0.2 (w:v) ratio. the mixture was stirred for 2 hours, then collected, filtered, and washed with ethanol before being dried at 70°C for 8 hours.

HNT acid treatment and caffeic acid loading

Caffeic acid loading into HNT was performed following a basic protocol adapted from several authors Garcia-Garcia *et al.* (2018); Prinz Setter & Segal. (2020) ; Satish *et al*. (2019), which involved mixing the nanotubes in a concentrated caffeic acid solution,

https://doi.org/10.1180/clm.2025.10013 Published online by Cambridge University Press

allowing efficient interaction between the nanotubes and the acid solution. To facilitate the infiltration of the caffeic acid into the HNT lumen, multiple vacuum cycles were applied, ensuring thorough penetration of the guest molecules. After infiltration, the mixture was subjected to centrifugation to separate unbound caffeic acid and remove excess solution. The nanotubes were then washed to eliminate any remaining impurities, followed by drying to obtain the caffeic acid loaded HNT. A critical step was carried out which is the selective etching of the lumen diameter using a mild acid treatment. In this case acetic acid was chosen for its etching properties without any structural integrity which effectively enhanced the inner surface area of the nanotubes, thereby improving the loading capacity (Garcia-Garcia *et al.*, 2017).

Characterisation techniques

Crystal structure of both modified and unmodified HNT was monitored by X-ray diffraction technique using a powder diffractometer Panalytical Empyrean at room temperature in reflection mode with an incident Cu-Ka radiation (k = 1.5405 Å) at 40 kV and 40 mA. The data were collected over Bragg angle (2θ) range of 5–70° with a scanning speed of 2° min^{-1}.

Crystalline domain size of HNT was estimated using the Scherrer equation (Boucenna *et al.*, 2023) [1], analysing the full width at half-maximum (FWHM) of the major diffraction peak:

$$L = 0.9\lambda / (2\Delta\theta \cos \theta) \quad [1]$$

Where L represents the crystallite size, λ is the X-ray wavelength (0.154 nm for Cu Kα radiation), Δθ is the FWHM of the diffraction peak, and θ is the angle of the peak.

https://doi.org/10.1180/clm.2025.10013 Published online by Cambridge University Press

Chemical composition of HNT before and after the corresponding treatments was obtained using a Bruker S8 Tiger WDXRF spectrometer, with a rhodium target X-ray tube operated at 50 kV.

Surface area and porosity of HNT were measured using a Quantachrome NOVA Touch 2LX analyser. Samples were degassed at 90 °C for 10 hours under vacuum prior to N_2 adsorption at 77 K. BET surface area and BJH pore volume were calculated using Nova Touch 2LX analyser.

Chemical structure changes were investigated through a Bruker Alpha spectrometer equipped with ATR module. Each sample was scanned over the range of 400–4000 cm^{-1} with 4 cm^{-1} resolution and 32 accumulated scans.

Surface morphology changes were examined using a JOEL 840 A LOGS scanning electron microscope (Tokyo, Japan) operated at 1–5 kV on metal-coated samples broken in liquid nitrogen.

Thermal stability was assessed using thermogravimetric analysis (TGA) with a PerkinElmer STA 6000 thermal analyser. Approximately 12 ± 0.5 mg of each sample were heated from 30°C to 800°C at 10°C.min^{-1} under a nitrogen atmosphere.

Results and discussion

Treatment effects on HNT crystal structure

The impact of HNT functionalisation on the crystal structure of both untreated and chemically treated HNT was examined. The X-ray diffraction (XRD) patterns of untreated HNT and those subjected to silane and caffeic acid treatment were analysed (Fig. 1).

The characteristic diffraction peaks of HNT at 2θ = 12.74° and 25.40°, corresponding to (001) and (002) diffraction planes with basal spacings of 7.35 Å and 3.44 Å respectively

https://doi.org/10.1180/clm.2025.10013 Published online by Cambridge University Press

signify the typical peaks of untreated HNT indicative of a dehydrated halloysite structure (7Å) (Chen *et al.*, 2018). The absence of a significant peak around 10 Å or another one migrating towards 8.5Å further confirmed the absence of the hydrated 10 Å form or the intermediate dehydrated state as was found by Liu *et al.* (2021); Siranidi *et al*. (2024). Additionally, the intense peak observed at 2θ = 20.70°, attributed to the (020) diffraction plane with a basal spacing of 3.89 Å, strongly supports the presence of tubular structure halloysite (Joussein *et al.*, 2007). The presence of manganese, responsible for the grey coloration of Algerian halloysite nanotubes, is evident from a peak at approximately 4 Å, with additional peaks indicate quartz and calcite impurities, common in natural HNT samples.

In the case of silane treatment, nearly identical peaks were observed in the XRD patterns of O-HNT, the crystalline form of HNT following OTES treatment remained intact. This preservation of crystalline structure is attributed to the robust hydrogen bonds between layers, which resist structural modification and provide stability resisting significant alteration even after chemical treatment. Furthermore, the intensity of these diffraction peaks diminishes progressively due to the delamination process induced by organic silane coating on the HNT surface that reduce the coherence of the crystalline lattice lowering intensities of peaks without shifting their positions, typically consistent with silane treated clay in the literature (Yuan *et al.*, 2008; He *et al.*, 2015).

Unlike the silane treatment, caffeic acid treatment resulted in a shift towards lower angles and an increase in intensity of HNT diffraction peaks, indicating the insertion of caffeic acid molecules between HNT interlayers and the disruption of tubular staking due to acid etching and internal loading (Wong *et al.*, 2021). This observation confirmed the successful loading of caffeic acid into the lumen and the chemical bonding with HNT functional groups.

https://doi.org/10.1180/clm.2025.10013 Published online by Cambridge University Press

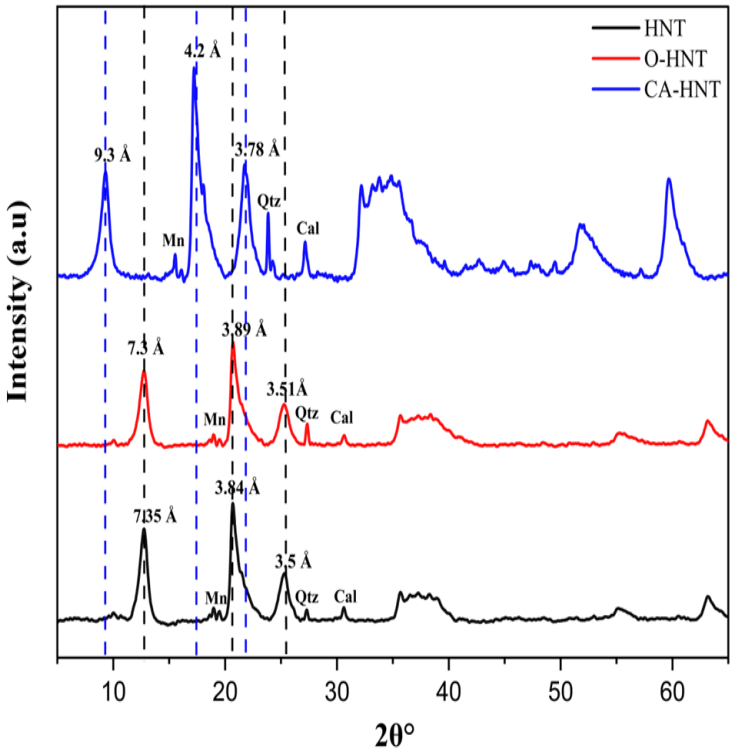

Figure 1. XRD pattern of untreated HNT and silanised HNT (O-HNT) with OTES and caffeic acid-loaded HNT (CA- HNT).

The crystallite size of untreated halloysite nanotubes (HNT), calculated using the Scherrer equation, was found to be 111.08 Å. Significant changes in crystallite size were observed following silane and caffeic acid treatments. Specifically, silane treatment reduced the crystallite size to 103Å. This decrease can be attributed to the formation of a surface coating on the nanotubes, likely due the silane organic alkyl chain grafting, which acts as a physical barrier that restricts the nucleation and growth of crystallites by limiting interlayer interactions and nucleation sites. In contrast, caffeic acid increased the crystallite size to 113.54 Å, which is thought to result from acid etching removing amorphous regions, permitting caffeic acid to interact with HNT functional groups and the formation of larger,

https://doi.org/10.1180/clm.2025.10013 Published online by Cambridge University Press

more defined crystalline structures within the nanotubes through chemical bonding within the lumen (Abdullayev *et al.*, 2012; Machowska *et al.*, 2022).

The observed changes similar in XRD patterns (Fig. 1), with diminished peak intensities after silane treatment, indicating smaller crystallites and delamination, while the shift to lower angles and increased intensities with caffeic acid reflect larger crystallites and structural enhancement. These results suggest that the diffraction behaviour is directly correlated with the crystal size variations, confirming the chemical modification impact on HNT. As the silane inhibits growth forming a surface barrier whereas, caffeic acid facilitates structural order through acid etching and interlayer interactions.

Treatment effects on HNT chemical composition

X-ray fluorescence (XRF) analysis was conducted to measure the concentrations of the major chemical elements in both untreated and chemically modified halloysite nanotubes (HNT) (Table 1). The analysis showed that the raw HNT consists of: SiO_2 (47.9 wt%) and Al_2O_3 (37.6 wt%) were silica and alumina are the predominant components, confirming the typical aluminosilicate composition of kaolinite-type halloysite structure (Stor *et al.*, 2023). Minor oxides including Fe_2O_3, SO_3, and ZnO were also detected.

Following silanization with OTES, the silica content increased to 49.1 wt% suggesting successful silane grafting, where the silane rich in silicon effectively coat the outer siloxane surface of HNT. Meanwhile, alumina decreased to 36.2 wt%, is attributed to the hydroxylation process, which led to partial alumina dissolution (Fu *et al.*, 2016).

Moreover, caffeic acid loading onto HNT decrease both Al_2O_3 and SiO_2 levels to 45.2 and 33.8 wt%, respectively, suggesting that a hydrophobic layer formed as evidenced by Garcia-Garcia *et al.* (2018). The reduction in alumina is also be attributed to the partial leaching of alumina cations from the octahedral layer due to acidic hydrolysis step with acetic

https://doi.org/10.1180/clm.2025.10013 Published online by Cambridge University Press

acid that primarily affects the inner surface (Sidorenko *et al.*, 2021), along with other trace elements.

Table 1. Chemical composition of HNT and treated HNT as obtained by XRF analysis.

Samples	Element content (wt%)								
	SiO_2	Al_2O_3	SO_3	Fe_2O_3	$CaCO_3$	CuO	ZnO	MnO_2	CoO
HNT	26.76	28.86	0.513	1.10	0.359	0.003	0.09	1.22	0.061
O-HNT	29.43	26.53	0.607	1.34	0.445	0.035	0.132	1.50	0.073
CA-HNT	24.37	23.61	0.539	0.987	0.076	0.003	0.072	0.793	0.047

These compositional changes align with the XRD results, supporting the conclusion that both surface treatments effectively induced selective modifications to halloysite nanotubes.

Treatment effect on HNT porous texture

The nitrogen adsorption-desorption isotherms of pristine HNT, O-HNT and CA-HNT (Fig. 2). According to IUPAC classification, the three samples display Type IV isotherms that correspond to mesoporous materials (Sangwichien & Aranovich, 2002). The hysteresis loops observed in the isotherms which are typical of type H3, suggesting that the pores are slit-shaped and associated with aggregates of plate-like particles. The hysteresis loops extend over the relative pressure (P/P_0) range of 0.4 to 1.0, indicative of capillary condensation within mesopores (pore width: 2–50 nm) (Panda *et al.*, 2010; Lim *et al.*, 2020).

https://doi.org/10.1180/clm.2025.10013 Published online by Cambridge University Press

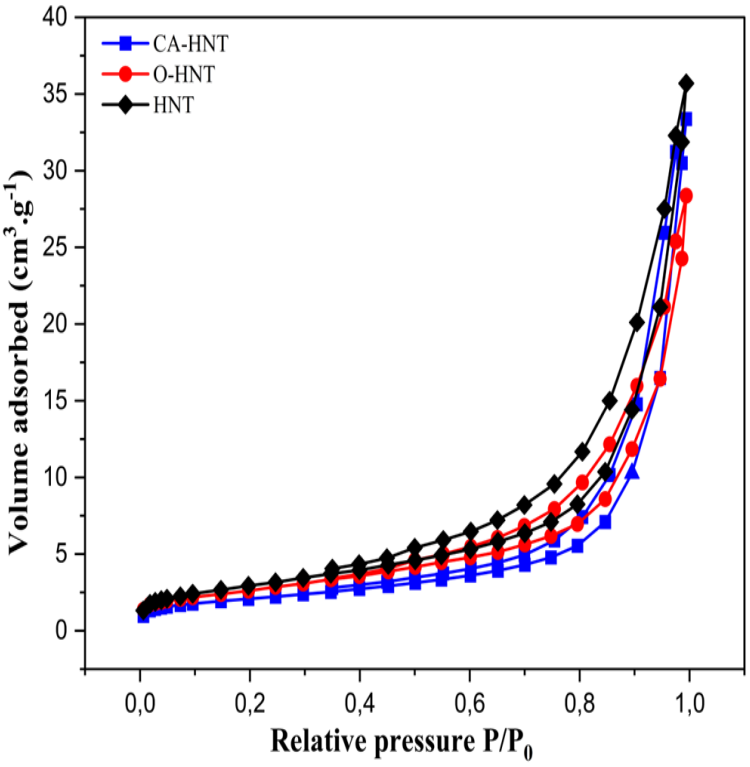

Figure 2. Nitrogen adsorption isotherms of untreated HNT and silanised HNT (O-HNT) with OTES and caffeic acid-loaded HNT (CA- HNT).

BET surface area and total pore volume of the untreated and modified HNT (Table 2 and Fig.3). Raw HNT exhibited a BET surface area of 54 $m^2.g^{-1}$ and a pore volume of 0.28 $cm^3.g^{-1}$, aligned with their natural tubular morphology and mesoporosity in the literature (Zhang *et al.*, 2012). After functionalisation with OTES silane agent, the surface area and pore volume increased significantly to 74 $m^2.g^{-1}$ and 0.341 $cm^3.g^{-1}$, respectively. This enhancement can be attributed to the improved dispersion of nanotubes and the exposure of previously inaccessible pores due to the silane moieties.

However, modification with caffeic acid resulted in a decrease in surface area measured at 42 $m^2.g^{-1}$ and an increasement in pore volume to 0.295 $cm^3.g^{-1}$. This reduction is possibly due to pore blocking caused by the deposition of caffeic acid molecules on the

https://doi.org/10.1180/clm.2025.10013 Published online by Cambridge University Press

surface edges and within the pores of the nanotubes. While, the increase is likely due to the acid etching widening the existing pores, which increases the volume capacity to hold guest molecules (Yu *et al.*, 2024).

Table 2. BET surface area and total pore volume of HNT, treated HNT with OTES and caffeic acid.

Sample	BET surface area ($m^2.g^{-1}$)	BJH total pore volume ($cm^{-3}.g^{-1}$)
HNT	54	0.281
O-HNT	74	0.341
CA-HNT	42	0.295

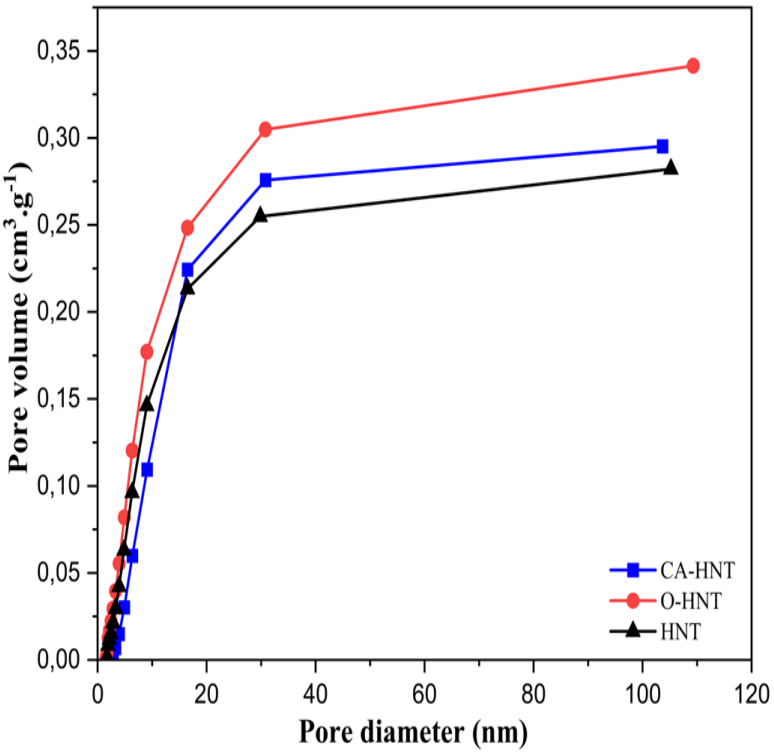

Figure 3. BJH total pore volume of untreated HNT and silanised HNT (O-HNT) with OTES and caffeic acid-loaded HNT (CA- HNT).

https://doi.org/10.1180/clm.2025.10013 Published online by Cambridge University Press

Across all samples, the BJH pore size distribution curves (Fig.4) reveal distinct alterations in textural properties, reflecting the effects of chemical modifications on the porous texture of halloysite nanotubes.

The untreated HNT sample exhibit a mesoporous nature with two distinct pore size distributions: a peak pore radius centered around 2 nm attributed to small internal and external pores alongside a broader peak at 8 to 10 nm, corresponding to the lumen consistent with the porosity arises predominantly from the lumen and surface defects (Pasbakhsh *et al.*, 2013).

The O-HNT sample, modified with triethoxy(octyl)silane (OTES), displays a shift in the peak pore radius toward 10–12 nm, suggests minor surface reorganization improvement due to the organosilane chain grafting, which likely removes surface impurities and reduces aggregation without significantly altering the pore structure leading to better enhanced compatibility in organic matrices.

The CA-HNT sample, initially subjected to acid etching with acetic acid step followed by caffeic acid loading, shows the most pronounced change, with a notable peak shifting further to 16 nm. The acid etching step with a weak acid as acetic acid, effectively removes structural impurities and mainly widens the already existing pores, promoting the macropore formatin through proton penetration induced dehydroxylation, and selective leaching of Al^{3+} cations from octahedral layers, creating larger voids in HNT matrice without introducing significant heterogeneity, thereby facilitating enhanced caffeic acid loading (Jauković *et al.*, 2021) unlike strong acids as sulphuric acid as Garcia-Garcia *et al.* (2017) reported which introduces heterogeneous porosity with multiple pore sizes peaks.

https://doi.org/10.1180/clm.2025.10013 Published online by Cambridge University Press

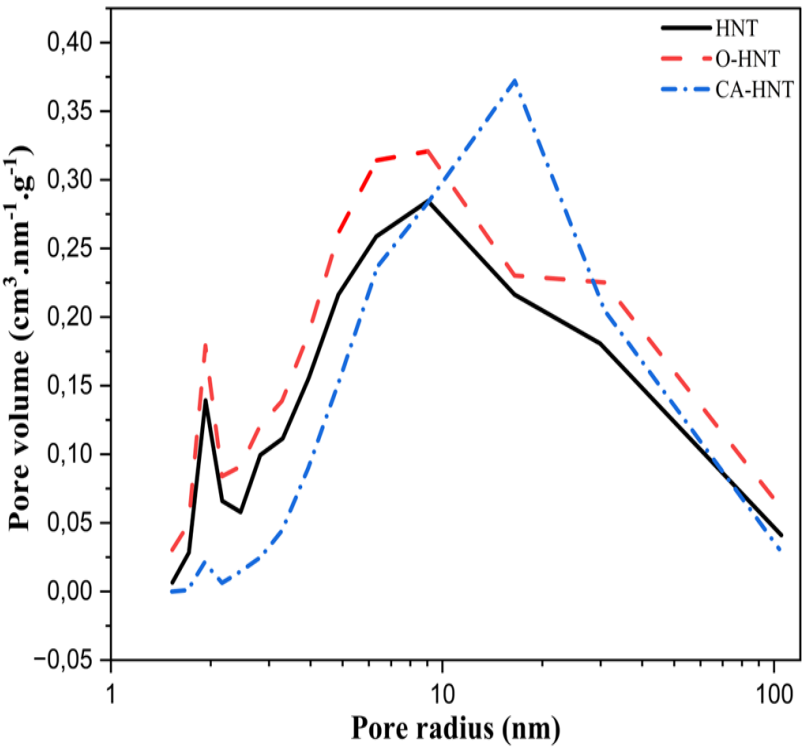

Figure 4. Pore size distribution of untreated HNT and silanised HNT (O-HNT) with OTES and caffeic acid-loaded HNT (CA- HNT).

Treatment Effects on HNT chemical structure

The spectrum of unmodified halloysite nanotubes (HNT) exhibits characteristic peaks at 3696, 3624, and 914 cm^{-1} corresponding to the stretching of inner-surface Al-OH, the stretching of inner Al-OH, and the bending vibration of inner Al-OH, respectively (Sabahi *et al.*, 2018). Peaks at 3456 and 1637 cm^{-1} relate to -OH stretching and bending vibration of adsorbed water. The appearance of 1637cm^{-1} peak or as it called zeolitic in palygorskite and sepiolite clays (Bukas *et al.*, 2013), suggested to be due the complete removal of residual bending water has not been achieved where it is found to be stuck in the defect sites or within the slit-like crevices formed during water loss according to Siranidi *et al.* (2024). Peaks at 1110, 1039, and 536 cm^{-1} are attributed to apical Si-O stretching vibration, in-plane Si-O stretching vibrations, and Si-O bending vibration, respectively. Additionally, peaks at 759

https://doi.org/10.1180/clm.2025.10013 Published online by Cambridge University Press

cm^{-1} and 686 cm^{-1} correspond to the symmetric stretching of Si-O-Si and the perpendicular stretching of Si-O-Al, respectively (Yuan *et al.*, 2008; Hillier *et al.*, 2016).

The spectrum of silanized HNT (O-HNT) (Fig. 5) shows a decrease in the peak of zeolitic water. This can be understood by considering that silanol groups, formed when the alkoxy groups in triethoxy(octyl)silane are hydrolyzed, interact with hydroxyl groups in the inner layers of HNT, as well as with the edges and surface defects on HNT. These interactions lead to a reduction in generating water that is subsequently removed during the drying process, possibly due to increased hydrophobicity of HNT after silanisation, limiting water adsorption, reducing the overall amount of adsorbed water between layers (Senyel & Dike, 2024b). Furthermore, new absorption bands appear in O-HNT, notably at 2922 cm^{-1} and 2852 cm^{-1}, attributed to the asymmetric and symmetric stretching vibration of aliphatic -CH groups beside the shifts and changes of peaks intensity, confirming the success of the silane treatment (Li *et al.*, 2015; Pal *et al.*, 2015).

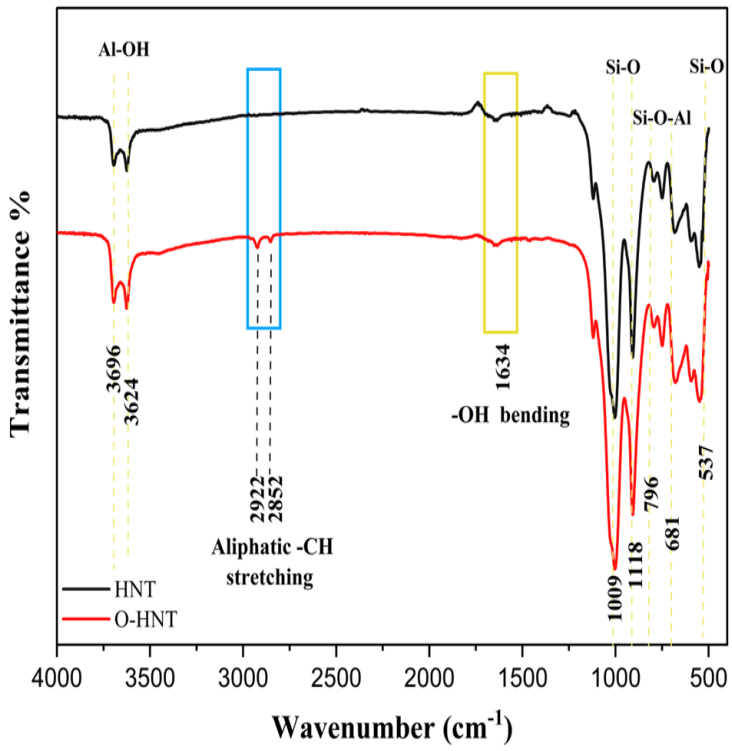

https://doi.org/10.1180/clm.2025.10013 Published online by Cambridge University Press

Figure 5. FTIR spectrum of untreated HNT, silanised HNT (O-HNT) with OTES.

However, upon treatment with caffeic acid and through a comparative analysis of the spectrum curves (Fig. 6) the emergence of new peaks becomes evident, notably around 1644, 1507, 1429, and 1294 cm^{-1}. These peaks are attributed to the C=O stretching, C=C stretching of aromatic ring group, -CH stretching of aromatic hydroxyl group and C-O phenolic stretching from caffeic acid (Arat & Uyanık 2017), respectively. Additionally, a noteworthy broader peak corresponding to the presence of phenolic –OH from caffeic acid at around 3400–3200 cm^{-1} is observed (Liu *et al.*, 2021). This serves as compelling evidence of the successful caffeic acid loading on HNT.

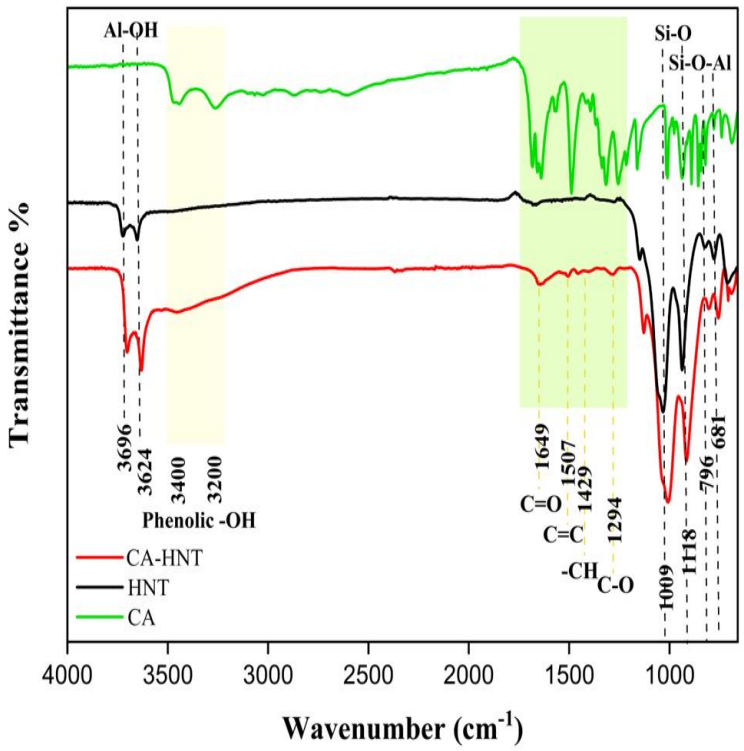

Figure 6. FTIR spectrum of untreated HNT, caffeic acid-loaded HNT (CA-HNT).

Treatment effects on HNT morphology

Scanning Electron Microscopy (SEM) morphological analysis indicates that pristine halloysite nanotubes (HNT) in Figure 7(a) exhibit well-defined tubular structures with

https://doi.org/10.1180/clm.2025.10013 Published online by Cambridge University Press

smooth, uniform, and consistent surfaces that tend to aggregate due to their hydrophilic nature which is typical of unmodified clays. This aggregation arises from the presence of hydroxyl groups.

Following treatment, the observed morphology changes noticeably upon O-HNT and CA-HNT samples in Figure 7(b and c) can be ascribed to the interaction between the hydroxyl moieties on HNT surface and the added OTES and caffeic acid compounds. O-HNT tubes appear to be aggregates with slightly roughened surfaces. This changes as Garcia-Garcia *et al.* (2018) described were attributed to silane molecules coated onto HNT external surfaces specifically through masking the nanotubes walls and edges due to the presence of silane organic moieties promoting surface roughness and decreasing hydrophilicity.

Furthermore, the analysis reveals that CA-HNT exhibit a rougher and more compact surface with an indistinct outline and noticeable sticking of nanotubes. This observation confirms a higher packing density of HNT aggregates, suggesting that the nanotubes are stacked or bundled more tightly (Zhang *et al.*, 2022). The loss of tube visibility with the increased density, indicating a significant alteration in their morphological characteristics compared to the unmodified HNT which can be attributed to the successful loading of caffeic acid.

Such modifications are expected to enhance the compatibility and homogeneity of the nanotubes as the morphological shape didn't get affected through the two process however their size and degree of agglomeration changed (Arat & Uyanık, 2017; Abu El-Soad *et al.*, 2020, 2021).

https://doi.org/10.1180/clm.2025.10013 Published online by Cambridge University Press

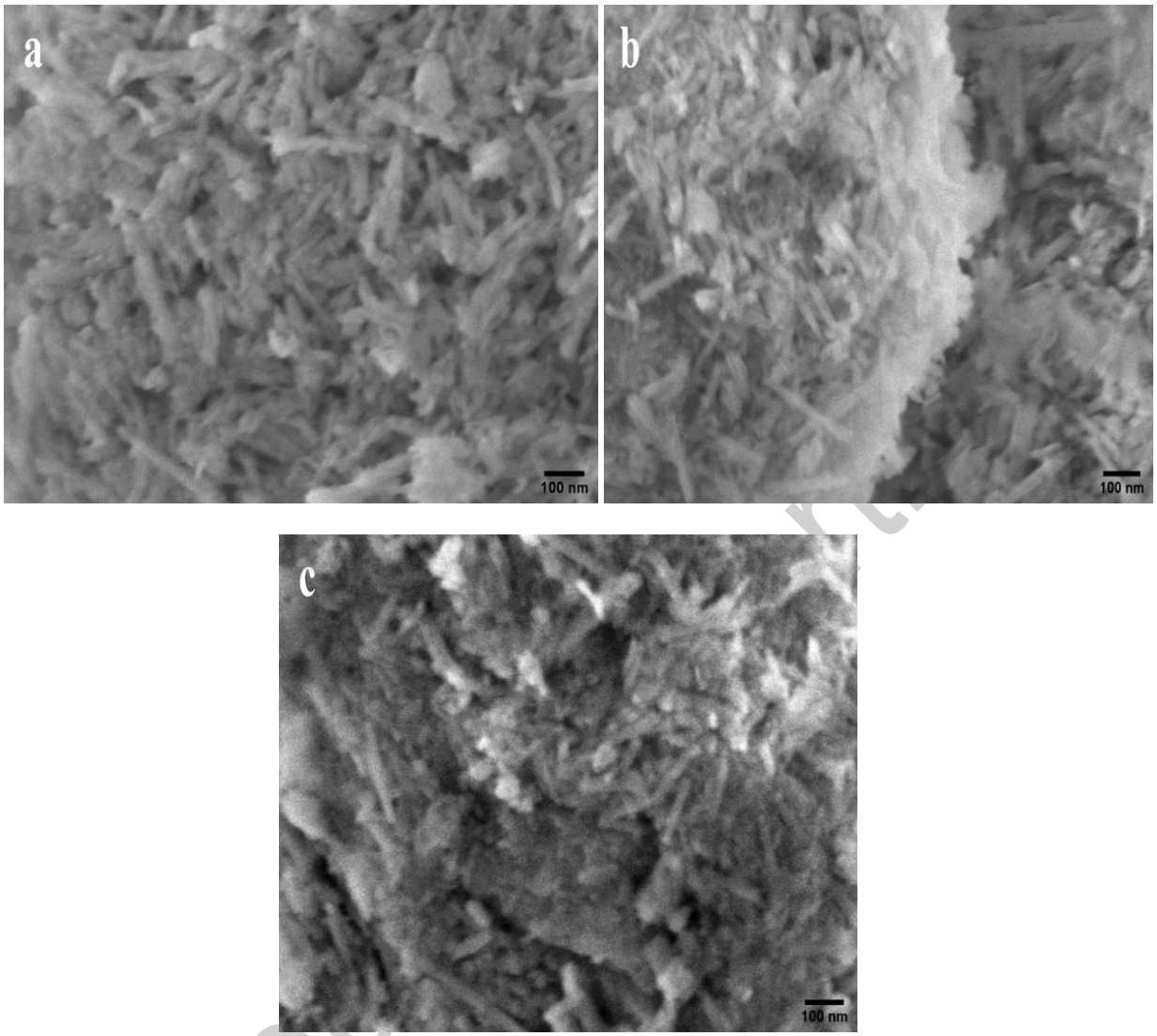

Figure 7. SEM images of (a) unmodified HNT (b) modified HNT with triethoxy(octyl)silane (O-HNT) and (c) HNT loaded with caffeic acid (CA-HNT).

Treatment effects on HNT thermal stability

Thermogravimetric Analysis (TGA) and Derivative Thermogravimetry (DTG) curves for both untreated and treated halloysite nanotubes (Fig. 8 and 9), providing crucial insights into their thermal degradation behaviour, the effects of modification with OTES and the loading efficiency of caffeic acid into HNT lumen.

https://doi.org/10.1180/clm.2025.10013 Published online by Cambridge University Press

Untreated HNT shows two distinct mass loss stages. Minor mass loss of 1.33%, occurs between 200-300 °C, attributed to the desorption of crystallisation water and adsorbed water from the surface and internal channels of the nanotubes. The second, more substantial mass loss of 12.76% between 400–600°C, with a DTG peak at 507°C, corresponds to the dihydroxylation of the structural Al-OH groups (Yu *et al.*, 2017; Abu El-Soad *et al.*, 2020).

Almost similar thermal behaviour is observed in organically modified HNT with triethoxy(octyl)silane, with slight yet significant differences. A reduction in crystallisation and adsorbed water mass to 1.22% is noted, which can be attributed to the hydrophobic nature of the silane treatment due to the long octyl alkyl chain extended from its triethoxy groups(Açışlı *et al.*, 2017; Rozhina *et al.*, 2020). Additionally, an increased mass loss estimated to 13.89% during dihydroxylation is observed, with slightly broadened DTG peak estimated at 501°C, likely due to gradual degradation of the organic compounds grafted onto the silane during the surface modification which serves as a determining factor in achieving less abrupt mass loss compared to HNT. The obtained results aligned with those reported in the literature (Belkassa *et al.*, 2013; Bischoff *et al.*, 2015). This implies that the graft of the organic moieties of the silane played a crucial role in modifying the surface chemistry, reducing the inherent hydrophilicity nature of HNT by promoting the dehydration process.

For CA-HNT case, notable variations in behaviour were identified compared to both HNT and O-HNT. Crystallisation and adsorbed water mass loss is no longer observed. A second reduced mass loss compared to HNT overall weight loss evaluated at 2.75% This stability is attributed HNT etching with acetic acid removing hydroxyl associated with thermal decomposition that is recorded between 400–600°C (Prinz Setter *et al.*, 2022), subsequently showing a shift in the decomposition peak at approximately 520°C (Liu *et al.*, 2018; Lim *et al.*, 2019). CA-HNT characterization was repeated three times to ensure the accuracy of these findings.

https://doi.org/10.1180/clm.2025.10013 Published online by Cambridge University Press

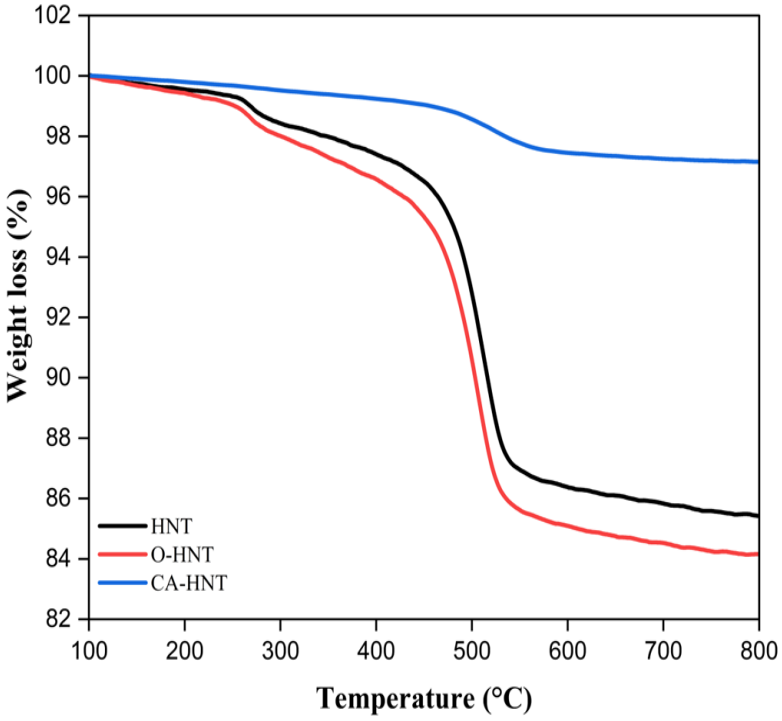

Figure 8. TGA of unmodified HNT and silanised HNT with OTES (O-HNT) and caffeic acid loaded HNT (CA-HNT).

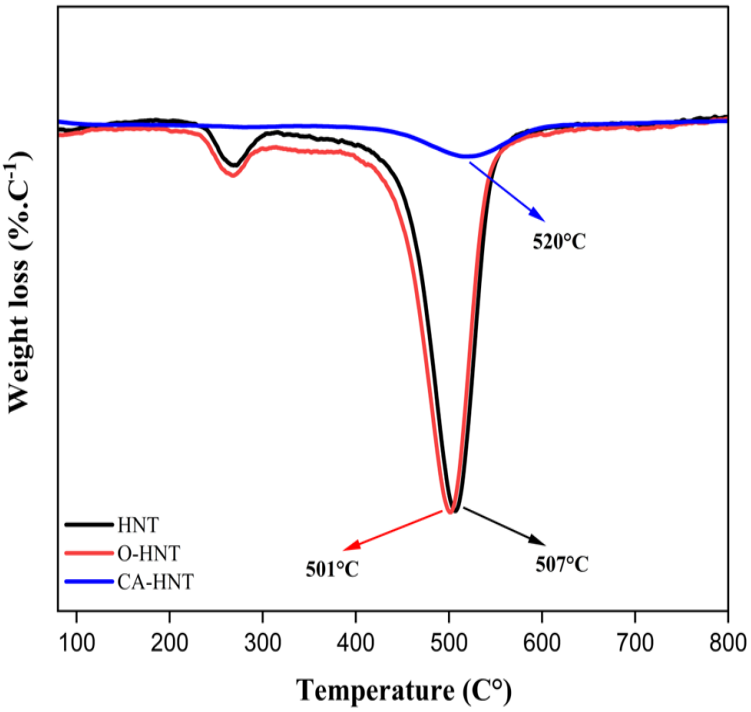

https://doi.org/10.1180/clm.2025.10013 Published online by Cambridge University Press

Figure 9. TGA of unmodified HNT and silanised HNT with OTES (O-HNT) and caffeic acid loaded HNT (CA-HNT).

The results suggest that the absence of caffeic acid decomposition, combined with reduced mass loss at decomposition stage, elimination of both crystallisation and adsorbed water along with an increase in degradation temperature with 13°C higher than pure HNT, indicated that loading of caffeic acid facilitated the elimination of water molecules as well effectively shielded halloysite nanotubes from heat-induced alterations, enhancing their thermal stability, however this enhancement was not that significant due to the small amount of caffeic acid loaded as justified by (Zahidah *et al.*, 2017). These findings align with the results of XRF, XRD, BET and FTIR analyses, which confirm the presence of caffeic acid either chemically bonded to HNT surface or encapsulated within the lumen. The lack of caffeic acid decomposition may be explained by the formation of a strong covalent bond between HNT and caffeic acid.

Conclusion

This research successfully demonstrated the functionalisation of Algerian halloysite nanotubes through two distinct methods: silanization with triethoxy(octyl)silane and caffeic acid loading.

These surface modifications were confirmed through comprehensive characterisation. XRD analysis showed that for OTES- HNT, the core crystalline structure remained intact, with a slight reduction in crystallite size and decreased peak intensities revealing the formation of a surface coating by the OTES moieties. Conversely, caffeic acid treatment led to an increase in crystallite size alongside noticeable shifts in the diffraction peaks, likely due to molecular interactions or subtle acid etching effects. XRF analysis revealed a higher silica content after silanization, while the caffeic acid treatment reduced both alumina and silica content due to acid etching, indicating successful surface modification and the formation of a

https://doi.org/10.1180/clm.2025.10013 Published online by Cambridge University Press

hydrophobic layer. FTIR analysis revealed new absorption bands unique to each grafted agent further confirming the chemical modifications. SEM analysis revealed that OTES treatment resulted in surface roughening, while caffeic acid led to a rougher, more compact, and tightly packed appearance of HNT aggregates, supporting successful grafting. TGA analysis revealed that OTES-HNT exhibited a reduction in initial adsorbed water loss (from 1.33% to 1.22%) and a slightly altered dehydroxylation profile (peak at 501°C). In contrast, CA-HNT demonstrated notably improved thermal stability by eliminating initial water loss and shifting their primary decomposition temperature to 520°C (13°C enhancement over pristine HNT), reporting enhanced resistance to degradation. BET analysis revealed that OTES treatment significantly increased the surface area from 54 m^2g^{-1} for pristine HNT to 74 m^2g^{-1}, while caffeic acid reduced it to 42 m^2g^{-1}, suggesting pore blocking by loaded molecules.

Overall, the modifications enhanced the properties of Algerian HNT by effectively preventing HNT aggregation and reducing their inherent hydrophilicity, which potentially leads to improved particle dispersion, compatibility with nonpolar matrices, and better thermal stability. This paves the way for modified HNT applications in advanced polymer nanocomposites, particularly in active packaging and thermal insulating materials, making them promising high-performance green nanofillers.

Authorship and contributorship

- Conceptualisation: Zeyneb Abir Mekhania
- Methodology: Zeyneb Abir Mekhania
- Investigation: Zeyneb Abir Mekhania, Nora Benkacher
- Visualisation: Zeyneb Abir Mekhania
- Writing – Original draft: Zeyneb Abir Mekhania
- Writing – Review and editing: Kahina Iggui, Aida Benhamida
- Supervision: Aida Benhamida, Kahina Iggui, Bengourna Nadjette

https://doi.org/10.1180/clm.2025.10013 Published online by Cambridge University Press

- Formal analysis: Kahina Iggui

- Data curation: Nora Benkacher, Abdelheq Layachi

- Project administration: Aida Benhamida, Bengourna Nadjette

- Data analysis: Atmane Djermoune, Farid Ait Merzeg, Abdelheq Layachi

- Validation: Atmane Djermoune, Farid Ait Merzeg

- Resources: Hamid Satha

Acknowledgements: The authors declare no acknowledgments.

Conflicts of interest: The authors declare none.

Funding: Not applicable.

References

Abdullayev E. & Joshi A. & Wei W. & Zhao Y. & Lvov Y. (2012) Enlargement of halloysite clay nanotube lumen by selective etching of aluminum oxide. *ACS Nano*, **6**, 7216–7226.

Abu El-Soad A.M. & Pestov A.V. & Tambasova D.P. & Osipova V.A. & Martemyanov N.A. & Cavallaro G. & Kovaleva E.G. & Lazzara G. (2020) Insights into grafting of (3-mercaptopropyl) trimethoxysilane on halloysite nanotubes surface. *Journal of Organometallic Chemistry*, **915**, 121224.

Abu El-Soad A.M. & Lazzara G. & Pestov A.V. & Tambasova D.P. & Antonov D.O. & Cavallaro G. & Kovaleva E.G. (2021) Grafting of (3-chloropropyl) -trimethoxysilane on halloysite nanotubes surface. *Applied Sciences*, **11**, 5530.

Açışlı Ö. & Karaca S. & Gürses A. (2017) Investigation of the alkyl chain lengths of surfactants on their adsorption by montmorillonite (Mt) from aqueous solutions. *Applied Clay Science*, **142**, 90–99.

Anbalagan G. & Sivakumar G. & Prabakaran S. & Gunasekaran S. (2010) Spectroscopic characterization of natural mineral halloysite. *Vibrational Spectroscopy*, **52**, 122–127.

https://doi.org/10.1180/clm.2025.10013 Published online by Cambridge University Press

Arat R. & Uyanık N. (2017) Surface modification of nanoclays with styrene-maleic anhydride copolymers. *Natural Resources*, **8**, 159–171.

Bao Z. & Yan Y. & Han W. (2024) Investigation of γ-aminopropyltriethoxysilane (APTES)-modified halloysite nanotubes on the reinforcement of halloysite/polypropylene (PP) nanocomposites. *Polymers*, **16**, 1114.

Belkassa K. & Bessaha F. & Marouf-Khelifa K. & Batonneau-Gener I. & Comparot J.D. & Khelifa A. (2013) Physicochemical and adsorptive properties of a heat-treated and acid-leached Algerian halloysite. *Colloids and Surfaces A: Physicochemical and Engineering Aspects*, **421**, 26–33.

Belver C. & Bañares Muñoz A.B. & Vicente M.A. (2002) Chemical activation of a kaolinite under acid and alkaline conditions. *Chemistry of Materials*, **14**, 2033–2043.

Biddeci G. & Cavallaro G. & Di Blasi F. & Lazzara G. & Massaro M. & Milioto S. & Parisi F. & Riela S. & Spinelli G. (2016) Halloysite nanotubes loaded with peppermint essential oil as filler for functional biopolymer film. *Carbohydrate Polymers*, **152**, 548–557.

Biddeci G. & Spinelli G. & Colomba P. & Di Blasi F. (2022a) Nanomaterials: a review about halloysite nanotubes, properties, and application in the biological field. *International Journal of Molecular Sciences*, **23**, 11518.

Biddeci G. & Spinelli G. & Colomba P. & Di Blasi F. (2022b) Nanomaterials: a review about halloysite nanotubes, properties, and application in the biological field. *International Journal of Molecular Sciences*, **23**, 11518.

Biddeci G. & Spinelli G. & Colomba P. & Di Blasi F. (2023) Halloysite nanotubes and sepiolite for health applications. *International Journal of Molecular Sciences*, **24**, 4801.

https://doi.org/10.1180/clm.2025.10013 Published online by Cambridge University Press

Bischoff E. & Daitx T. & Simon D.A. & Schrekker H.S. & Liberman S.A. & Mauler R.S. (2015) Organosilane-functionalized halloysite for high performance halloysite/heterophasic ethylene-propylene copolymer nanocomposites. *Applied Clay Science*, **112–113**, 68–74.

Boccalon E. & Sassi P. & Pioppi L. & Ricci A. & Marinozzi M. & Gorrasi G. & Nocchetti M. (2022) Onion skin extract immobilized on halloysite-layered double hydroxide filler as active pH indicator for food packaging. *Applied Clay Science*, **227**, 106611.

Boucenna Y. & Layachi A. & Cherfia A. & Laoutid F. & Satha H. (2023) Non-isothermal crystallization kinetics and activation energy for crystal growth of polyamide 66/short glass fiber/carbon black composites. *Materials*, **16**, 2034.

Brindley G.W. & Brown G., editors (1980) *Crystal structure of clay minerals and their X-ray identification*. Mineralogical Society, London, UK, 504 pp.

Bugatti V. & Sorrentino A. & Gorrasi G. (2017) Encapsulation of lysozyme into halloysite nanotubes and dispersion in PLA : structural and physical properties and controlled release analysis. *European Polymer Journal*, **93**, 495–506.

Bukas V.J. & Tsampodimou M. & Gionis V. & Chryssikos G.D. (2013) Synchronous ATR infrared and NIR-spectroscopy investigation of sepiolite upon drying. *Vibrational Spectroscopy*, **68**, 51–60.

Butun Sengel S. & Tunca N. & Deveci H. & Bas H. & Butun V. (2023) Smart materials and their advanced biomedical applications : HNT and HNT-polymer composites. *Smart Materials in Medicine*, **4**, 955–974.

Çankaya N. & Ünal A. & Korcan S.E. (2024) Comparison of the antimicrobial and antioxidant properties of halloysite nanotubes and organoclays as green source materials. *Clay Minerals*, **59**, 1–10.

https://doi.org/10.1180/clm.2025.10013 Published online by Cambridge University Press

Carli L.N. & Daitx T.S. & Soares G.V. & Crespo J.S. & Mauler R.S. (2014) The effects of silane coupling agents on the properties of PHBV/halloysite nanocomposites. *Applied Clay Science*, **87**, 311–319.

Chen S. & Yang Z. & Wang F. (2018) Investigation on the properties of PMMA/reactive halloysite nanocomposites based on halloysite with double bonds. *Polymers*, **10**, 1038.

Cheng Z.-L. & Chang X.-Y. & Liu Z. & Qin D.-Z. & Zhu A.-P. (2017) High-performance PTFE nanocomposites based on halloysite nanotubes. *Clay Minerals*, **52**, 427–438.

Elmi C. (2023) Physical-chemical properties of nano-sized phyllosilicates : recent environmental and industrial advancements. *Encyclopedia*, **3**, 1439–1460.

Fahimizadeh M. & Wong L.W. & Baifa Z. & Sadjadi S. & Auckloo S.A.B. & Palaniandy K. & Pasbakhsh P. & Tan J.B.L. & Singh R.K.R. & Yuan P. (2024) Halloysite clay nanotubes : innovative applications by smart systems. *Applied Clay Science*, **256**, 107423.

Fu H. & Wang Y. & Li X. & Chen W. (2016) Synthesis of vegetable oil-based waterborne polyurethane/silver-halloysite antibacterial nanocomposites. *Composites Science and Technology*, **126**, 86–93.

Gaaz T.S. & Sulong A.B. & Kadhum A.A.H. & Al-Amiery A.A. & Nassir M.H. & Jaaz A.H. (2017) The impact of halloysite on the thermo-mechanical properties of polymer composites. *Molecules*, **22**, 838.

Ganapathy D. & Shanmugam R. & Pitchiah S. & Murugan P. & Chinnathambi A. & Alharbi S.A. & Durairaj K. & Sundramoorthy A.K. (2022) Potential applications of halloysite nanotubes as drug carriers : a review. *Journal of Nanomaterials*, **2022**, 8182967.

https://doi.org/10.1180/clm.2025.10013 Published online by Cambridge University Press

Garcia-Garcia D. & Ferri J.M. & Ripoll L. & Hidalgo M. & Lopez-Martinez J. & Balart R. (2017) Characterization of selectively etched halloysite nanotubes by acid treatment. *Applied Surface Science*, **422**, 616–625.

Garcia-Garcia D. & Garcia-Sanoguera D. & Fombuena V. & Lopez-Martinez J. & Balart R. (2018) Improvement of mechanical and thermal properties of poly(3-hydroxybutyrate) (PHB) blends with surface-modified halloysite nanotubes (HNT). *Applied Clay Science*, **162**, 487–498.

Guo F. & Aryana S. & Han Y. & Jiao Y. (2018) A review of the synthesis and applications of polymer-nanoclay composites. *Applied Sciences*, **8**, 1696.

He Y. & Xu W. & Tang R. & Zhang C. & Yang Q. (2015) pH-responsive nanovalves based on encapsulated halloysite for the controlled release of a corrosion inhibitor in epoxy coating. *RSC Advances*, **5**, 90609–90620.

Hillier S. & Brydson R. & Delbos E. & Fraser T. & Gray N. & Pendlowski H. & Phillips I. & Robertson J. & Wilson I. (2016) Correlations among the mineralogical and physical properties of halloysite nanotubes (HNTs). *Clay Minerals*, **51**, 325–350.

Jafazadeh S. & Haddadi-Asl V. (2023) Surface modification of halloysite nanotube with an amine terminated block copolymer. *Research Square*, doi:10.21203/rs.3.rs-2993656/v1.

Jauković V. & Krajišnik D. & Daković A. & Damjanović A. & Krstić J. & Stojanović J. & Čalija B. (2021) Influence of selective acid-etching on functionality of halloysite-chitosan nanocontainers for sustained drug release. *Materials Science and Engineering C*, **123**, 111973.

https://doi.org/10.1180/clm.2025.10013 Published online by Cambridge University Press

Jawwad Saif M. & Muhammad Asif H. & Naveed M. (2018) Properties and modification methods of halloysite nanotubes : a state-of-the-art review. *Journal of Nanomaterials*, **2018**, 3450296.

Joussein E. & Petit S. & Delvaux B. (2007) Behavior of halloysite clay under formamide treatment. *Applied Clay Science*, **35**, 17–24.

Kassa A. & Benhamida A. & Kaci M. & Bruzaud S. (2020) Effects of montmorillonite, sepiolite, and halloysite clays on the morphology and properties of polycaprolactone bionanocomposites. *Polymers and Polymer Composites*, **28**, 338–347.

Katuwavila N.P. & Perera A.D.L.C. & Karunaratne V. & Amaratunga G.A.J. & Karunaratne D.N. (2016) Improved delivery of caffeic acid through liposomal encapsulation. *Journal of Nanomaterials*, **2016**, 9701870.

Kaur G. & Gupta S. & Prakash V. & Rodriguez R.D. & Sheremet E. & Mehta S.K. & Sharma S. (2024) A comprehensive review of varied applications of modified halloysite nanocomposites. *Nano-Structures & Nano-Objects*, **39**, 101230.

Kennouche S. & Le Moigne N. & Kaci M. & Quantin J.-C. & Caro-Bretelle A.-S. & Delaite C. & Lopez-Cuesta J.-M. & Caro A.-S. (2016) Morphological characterization and thermal properties of compatibilized poly(3-hydroxybutyrate-co-3-hydroxyvalerate) (PHBV)/poly(butylene succinate) (PBS)/halloysite ternary nanocomposites. *European Polymer Journal*, **75**, 142–162.

Kim J.H. & Kim H.J. & Lee D. & Yang S.B. & Yu S. & Kim H.G. & Seo B. & Nam S.Y. & Lim H.J. & Lim C.S. & Kwon D.J. (2025) Improvement adhesion durability of epoxy adhesive for steel/carbon fiber-reinforced polymer adhesive joint using imidazole-treated halloysite nanotube. *Advanced Composites and Hybrid Materials*, **8**, 29.

https://doi.org/10.1180/clm.2025.10013 Published online by Cambridge University Press

Kokulnathan T. & Wang T.J. & Thangapandian M. & Alaswad S.O. (2020) Synthesis and characterization of hexagonal boron nitride/halloysite nanoparticles for biomedical applications. *Applied Clay Science*, **187**, 105477.

Kouser S.L. & Sheik S.K. & Nagaraja G.K. & Prabhu A. & Prashantha K. & D'souza A.M. & Navada K.M. & Manasa D.J. (2020) Functionalization of halloysite nanoparticles with chitosan reinforced poly (vinyl alcohol) for potential biomedical applications. *International Journal of Molecular Sciences*, **165**, 1079–1092.

Kouser L.S. & Prabhu A. & Prashantha K. & Nagaraja G.K. & D'souza A.M. & Meghana Navada K. & Qurashi A. & Manasa D.J. (2022) Modified halloysite nanoparticles with chitosan incorporated PVA/PVP bionanocomposite films : thermal, mechanical properties and biocompatibility for tissue engineering. *Colloids and Surfaces A : Physicochemical and Engineering Aspects*, **634**, 127977.

Lazzara G. & Cavallaro G. & Panchal A. & Fakhrullin R. & Stavitskaya A. & Vinokurov V. & Lvov Y. (2018) An assembly of organic-inorganic composites using halloysite clay nanoparticles. *Current Opinion in Colloid and Interface Science*, **35**, 42–50.

Lei X. & Zhou Y. & Liu X. & Kong L. & Liao L. & Li Y. & Liu M. & Tian L. & Rao W. & Lv G. (2023) Effective pH-responsive nanocarrier based on the anisotropic surfaces of halloysite nanoparticles for controlled drug release. *Applied Clay Science*, **232**, 106789.

Li H. & Zhu X. & Zhou H. & Zhong S. (2015) Functionalization of halloysite nanoparticles by enlargement and hydrophobicity for sustained release of analgesic. *Colloids and Surfaces A : Physicochemical and Engineering Aspects*, **487**, 154–161.

Lim K. & Chow W.S. & Pung S.Y. (2019) Enhancement of thermal stability and UV resistance of halloysite nanoparticles using zinc oxide functionalization via a solvent-free approach. *International Journal of Minerals, Metallurgy and Materials*, **26**, 787–795.

https://doi.org/10.1180/clm.2025.10013 Published online by Cambridge University Press

Lim S. & Park S. & Sohn D. (2020) Modification of halloysite nanoparticles for enhancement of gas-adsorption capacity. *Clays and Clay Minerals*, **68**, 189–196.

Lisuzzo L. & Cavallaro G. & Milioto S. & Lazzara G. (2020) Effects of halloysite content on the thermo-mechanical performances of composite bioplastics. *Applied Clay Science*, **185**, 105416.

Lisuzzo L. & Bertini M. & Lazzara G. & Ferlito C. & Ferrante F. & Duca D. (2023) A computational and experimental investigation of the anchoring of organosilanes on the halloysite silicic surface. *Applied Clay Science*, **245**, 107133.

Liu J. & Wang X. & Bai R. & Zhang N. & Kan J. & Jin C. (2018) Synthesis, characterization, and antioxidant activity of caffeic-acid-grafted corn starch. *Starch/Staerke*, **70**, 1700298.

Liu M. & Jia Z. & Jia D. & Zhou C. (2014) Recent advance in research on halloysite nanoparticles-polymer nanocomposite. *Progress in Polymer Science*, **39**, 1498–1525.

Liu S.T. & Chen X.G. & Zhang S.L. & Liu X.M. & Zhang J.J. (2021) Preparation and characterization of halloysite-based carriers for quercetin loading and release. *Clays and Clay Minerals*, **69**, 94–104.

Ma W. & Wu H. & Higaki Y. & Takahara A. (2018) Halloysite nanoparticles: green nanomaterial for functional organic-inorganic nanohybrids. *Chemical Record*, **18**, 986–999.

Machowska A. & Klara J. & Ledwójcik G. & Wójcik K. & Dulińska-Litewka J. & Karewicz A. (2022) Clindamycin-loaded halloysite nanoparticles as the antibacterial component of composite hydrogel for bone repair. *Polymers*, **14**, 2341.

Massaro M. & Noto R. & Riela S. (2022a) Halloysite nanoparticles: smart nanomaterials in catalysis. *Catalysts*, **12**, 149.

https://doi.org/10.1180/clm.2025.10013 Published online by Cambridge University Press

Massaro M. & Licandro E. & Cauteruccio S. & Lazzara G. & Liotta L.F. & Notarbartolo M. & Raymo F.M. & Sánchez-Espejo R. & Viseras-Iborra C. & Riela S. (2022b) Nanocarrier based on halloysite and fluorescent probe for intracellular delivery of peptide nucleic acids. *Journal of Colloid and Interface Science*, **620**, 221–233.

Maurya D.K. & Devasagayam T.P.A. (2010) Antioxidant and prooxidant nature of hydroxycinnamic acid derivatives ferulic and caffeic acids. *Food and Chemical Toxicology*, **48**, 3369–3373.

Meng Y. & Wang M. & Tang M. & Hong G. & Gao J. & Chen Y. (2017) Preparation of robust superhydrophobic halloysite clay nanoparticles via mussel-inspired surface modification. *Applied Sciences*, **7**, 1129.

Nazir M.S. & Mohamad Kassim M.H. & Mohapatra L. & Gilani M.A. & Raza M.R. & Majeed K. (2016) Characteristic properties of nanoclays and characterization of nanoparticulates and nanocomposites. Pp. 35–55 in: *Nanoclay reinforced polymer composites* (M. Jawaid & A.E.H. Oualid, editors). Springer, Singapore.

Ouyang J. & Liu T. & Yang H. & Zhang Y. (2019) Multiple polarization loss and permittivity adjusting of halloysite/BN co-doped carbon/cobalt composites. *Journal of Colloid and Interface Science*, **555**, 509–518.

Pal P. & Kundu M.K. & Malas A. & Das C.K. (2015) Thermo mechanical properties of organically modified halloysite nanoparticles/cyclic olefin copolymer composite. *Polymer Composites*, **36**, 955–960.

Panda A.K. & Mishra B.G. & Mishra D.K. & Singh R.K. (2010) Effect of sulphuric acid treatment on the physico-chemical characteristics of kaolin clay. *Colloids and Surfaces A: Physicochemical and Engineering Aspects*, **363**, 98–104.

https://doi.org/10.1180/clm.2025.10013 Published online by Cambridge University Press

Pasbakhsh P. & Churchman G.J. & Keeling J.L. (2013) Characterisation of properties of various halloysites relevant to their use as nanoparticles and microfibre fillers. *Applied Clay Science*, **74**, 47–57.

Petková M. & Ryba J. & Hrabovská V. & Ujhelyiová A. & Hricová M. (2019) The crystallization of polypropylene/halloysite fibers. *Journal of Thermal Analysis and Calorimetry*, **136**, 1093–1101. Prinz Setter O. (2020) Halloysite nanoparticles-the nano-bio interface. *Nanoscale*, **12**, 23444–23460.

Prinz Setter O. & Dahan L. & Abu Hamad H. & Segal E. (2022) Acid-etched halloysite nanoparticles as superior carriers for ciprofloxacin. *Applied Clay Science*, **228**, 106627.

Prishchenko D.A. & Zenkov E.V. & Mazurenko V.V. & Fakhrullin R.F. & Lvov Y.M. & Mazurenko V.G. (2018) Molecular dynamics of the halloysite nanoparticles. *Physical Chemistry Chemical Physics*, **20**, 5841–5849.

Qin L. & Dong G. & Nie Y. & Fakhrullin R. & Zhang B. & Zhang Y. (2024) Progress in design of halloysite nanoparticles-polymer nanocomposite membranes and their applications. *Advanced Membranes*, **4**, 100091.

Rawtani D. & Phd M.E. & Agrawal Y.K. (2012) Multifarious applications of halloysite nanoparticles: a review. *Reviews in Advanced Sciences and Engineering*, **1**, 282–295.

Rawtani D. & Pandey G. & Tharmavaram M. & Pathak P. & Akkireddy S. & Agrawal Y.K. (2017) Development of a novel ‘nanocarrier’ system based on halloysite nanoparticles to overcome the complexation of ciprofloxacin with iron: an in vitro approach. *Applied Clay Science*, **150**, 293–302.

https://doi.org/10.1180/clm.2025.10013 Published online by Cambridge University Press

Rozhina E. & Panchal A. & Akhatova F. & Lvov Y. & Fakhrullin R. (2020) Cytocompatibility and cellular uptake of alkylsilane-modified hydrophobic halloysite nanoparticles. *Applied Clay Science*, **185**, 105413.

Sabahi H. & Khorami M. & Rezayan A.H. & Jafari Y. & Karami M.H. (2018) Surface functionalization of halloysite nanoparticles via curcumin inclusion. *Colloids and Surfaces A: Physicochemical and Engineering Aspects*, **538**, 834–840. Sadjadi S. (2020) Halloysite-based hybrids/composites in catalysis. *Applied Clay Science*, **189**, 105537.

Sahnoune M. & Taguet A. & Otazaghine B. & Kaci M. & Lopez-Cuesta J.-M. (2017) Effects of functionalized halloysite on morphology and properties of polyamide 11/SEBS-g-MA blends. *Polymer International*, **66**, 1160–1167.

Sánchez-Fernández A. & Peña-Parás L. & Vidaltamayo R. & Cué-Sampedro R. & Mendoza-Martínez A. & Zomosa-Signoret V.C. & Rivas-Estilla A.M. & Riojas P. (2014) Synthesization, characterization, and in vitro evaluation of cytotoxicity of biomaterials based on halloysite nanoparticles. *Materials*, **7**, 7770–7780.

Sangwichien C. & Aranovich G. (2002) Density functional theory predictions of adsorption isotherms with hysteresis loops. *Physical Review E*, **66**, 313–320.

Santos A.C. & Ferreira C. & Veiga F. & Ribeiro A.J. & Panchal A. & Lvov Y. & Agarwal A. (2018) Halloysite clay nanoparticles for life sciences applications: from drug encapsulation to bioscaffold. *Advances in Colloid and Interface Science*, **257**, 58–70.

Sargazi S. & Laraib U. & Barani M. & Rahdar A. & Fatima I. & Bilal M. & Pandey S. & Sharma R.K. & Kyzas G.Z. (2022) Recent trends in mesoporous silica nanoparticles of rode-like morphology for cancer theranostics: a review. *Journal of Molecular Structure*, **1261**, 132870.

https://doi.org/10.1180/clm.2025.10013 Published online by Cambridge University Press

Satish S. & Tharmavaram M. & Rawtani D. (2019) Halloysite nanoparticles as a nature's boon for biomedical applications. *BJGP Open*, **6**, 100071.

Senyel M. & Dike A.S. (2024a) Contribution of silane modification of halloysite nanoparticle to its poly(butylene terephthalate)-based nanocomposites : structural, mechanical and thermal properties. *Polymer Bulletin*, **81**, 9851–9870.

Senyel M. & Dike A.S. (2024b) Contribution of silane modification of halloysite nanoparticle to its poly (butylene terephthalate)-based nanocomposites : structural, mechanical and thermal properties. *Polymer Bulletin*, **81**, 9851–9870.

Sidorenko A.Y. & Kurban Y.M. & Aho A. & Ihnatovich Z.V. & Kuznetsova T.F. & Heinmaa I. & Murzin D.Y. & Agabekov V.E. (2021) Solvent-free synthesis of tetrahydropyran alcohols over acid-modified clays. *Molecular Catalysis*, **499**, 111297.

Siranidi E. & Hillier S. & Chryssikos G.D. (2024a) Structure of tubular halloysite-(10 Å) and its transition to halloysite-(7 Å) by infrared spectroscopy and X-ray diffraction. *Clays and Clay Minerals*, **72**, e5.

Siranidi E. & Hillier S. & Chryssikos G.D. (2024b) Structure of tubular halloysite-(10 Å) and its transition to halloysite-(7 Å) by infrared spectroscopy and X-ray diffraction. *Clays and Clay Minerals*, **72**, e5.

Siy B.S.C. & Tan J.A.X.C. & Viron K.P. & Sajor N.J.B. & Santos G.N.C. & Penaloza D.P. (2020) Application of silane coupling agents to abaca fibers for hydrophobic modification. *Cellulose Chemistry and Technology*, **54**, 365–369.

Stor M. & Czelej K. & Krasiński A. & Gradoń L. (2023) Exceptional sorption of heavy metals from natural water by halloysite particles: a new prospect of highly efficient water remediation. *Nanomaterials*, **13**, 1968.

https://doi.org/10.1180/clm.2025.10013 Published online by Cambridge University Press

Sun P. & Liu G. & Lv D. & Dong X. & Wu J. & Wang D. (2015) Effective activation of halloysite nanoparticles by piranha solution for amine modification via silane coupling chemistry. *RSC Advances*, **5**, 52916–52925.

Sun Y. & Yu B. & Liu Y. & Yan J. & Xu Z. & Cheng B. & Huang F. & Wang J. (2024) Bio-inspired surface manipulation of halloysite nanoparticles for high-performance flame retardant polylactic acid nanocomposites. *Nano Research*, **17**, 1595–1606.

Tarasova E. & Naumenko E. & Rozhina E. & Akhatova F. & Fakhrullin R. (2019) Cytocompatibility and uptake of polycations-modified halloysite clay nanoparticles. *Applied Clay Science*, **169**, 21–30.

Taroni T. & Meroni D. & Fidecka K. & Maggioni D. & Longhi M. & Ardizzone S. (2019) Halloysite nanoparticles functionalization with phosphonic acids: role of surface charge on molecule localization and reversibility. *Applied Surface Science*, **486**, 466–473.

Tharmavaram M. & Pandey G. & Rawtani D. (2018) Surface modified halloysite nanoparticles: a flexible interface for biological, environmental and catalytic applications. *Advances in Colloid and Interface Science*, **261**, 82–101.

Wieczorek M. & Tatarchuk T. & Skórczewska K. & Szulc J. & Tomaszewska J. (2024) The effect of silanized halloysite nanoparticles on the structure of polyethylene-based composite. *Materials*, **17**, 2651.

Wong L.W. & Pasbakhsh P. & Arabi A.M. & Keeling J. & Tan J.B.L. (2021) Halloysite nanoparticles from various geological deposits: new insights to acid etching and their impacts on products' characteristics. *Journal of Environmental Chemical Engineering*, **9**, 106127.

https://doi.org/10.1180/clm.2025.10013 Published online by Cambridge University Press

Yang Y. & Chen Y. & Leng F. & Huang L. & Wang Z. & Tian W. (2017) Recent advances on surface modification of halloysite nanoparticles for multifunctional applications. *Applied Sciences*, **7**, 1215.

Yu D. & Wang J. & Hu W. & Guo R. (2017) Preparation and controlled release behavior of halloysite/2-mercaptobenzothiazole nanocomposite with calcined halloysite as nanocontainer. *Materials and Design*, **129**, 103–110.

Yu H. & Xu H. & Hao T. & Yuan Y. & Zhang B. & Wang H. & Shao G. & Fan B. & Lu H. (2024) Facile synthesis of ZnO/halloysite nanoparticle composite with greatly enhanced photocatalytic performance. *Colloids and Surfaces A: Physicochemical and Engineering Aspects*, **688**, 133575.

Yuan P. & Southon P.D. & Liu Z. & Green M.E.R. & Hook J.M. & Antill S.J. & Kepert C.J. (2008) Functionalization of halloysite clay nanoparticles by grafting with γ-aminopropyltriethoxysilane. *Journal of Physical Chemistry C*, **112**, 15742–15751.

Yuan P. & Tan D. & Annabi-Bergaya F. (2015) Properties and applications of halloysite nanoparticles: recent research advances and futurs prospects. *Applied Clay Science*, **112–113**, 75–93.

Zahidah K.A. & Raja B. & Kakooei S. & Kermanioryani M. & Mohebbi H. & Ismail M.C. & Bothi Raja P. (2017) Benzimidazole-loaded halloysite nanoparticle as a smart coating application. *Progress in Organic Coatings*, **111**, 243–254.

Zhang A.B. & Pan L. & Zhang H.Y. & Liu S.T. & Ye Y. & Xia M.S. & Chen X.G. (2012) Effects of acid treatment on the physico-chemical and pore characteristics of halloysite. *Colloids and Surfaces A : Physicochemical and Engineering Aspects*, **396**, 182–188.

https://doi.org/10.1180/clm.2025.10013 Published online by Cambridge University Press

Zhang H. (2017) Selective modification of inner surface of halloysite nanoparticles: a review. *Nanotechnology Reviews*, **6**, 573–581.

Zhang J. & Huang Z. & Yang M. & Dong S. & Zhou F. & Yan C. & Hu Y. & Yang H. & Gao Y. (2025a) Halloysite nanoparticles potentiate protein assembly for facile fabrication of nanocomposite thin film and its application in wound dressing. *Applied Clay Science*, **272**, 107260.

Zhang J. & Huang Z. & Yang M. & Dong S. & Zhou F. & Yan C. & Hu Y. & Yang H. & Gao Y. (2025b) Halloysite nanoparticles potentiate protein assembly for facile fabrication of nanocomposite thin film and its application in wound dressing. *Applied Clay Science*, **272**, 107260.

Zhang Y. & Tang A. & Yang H. & Ouyang J. (2016) Applications and interfaces of halloysite nanocomposites. *Applied Clay Science*, **114**, 530–548.

Zhang Y. & Meng R. & Zhou J. & Liu X. & Guo W. (2022) Halloysite nanoparticles-decorated electrospun biobased polyamide scaffolds for tissue engineering applications. *Colloids and Surfaces A : Physicochemical and Engineering Aspects*, **648**, 129385.

Zhao X. & Zhou C. & Liu M. (2020) Self-assembled structures of halloysite nanoparticles: towards the development of high-performance biomedical materials. *Journal of Materials Chemistry B*, **8**, 838–851.

Figures Captions

Figure 1. XRD pattern of untreated HNT and silanised HNT (O-HNT) with OTES and caffeic acid-loaded HNT (CA- HNT).

Figure 2. Nitrogen adsorption isotherms of untreated HNT and silanised HNT (O-HNT) with OTES and caffeic acid-loaded HNT (CA- HNT).

https://doi.org/10.1180/clm.2025.10013 Published online by Cambridge University Press

Figure 3. BJH total pore volume of untreated HNT and silanised HNT (O-HNT) with OTES and caffeic acid-loaded HNT (CA- HNT).

Figure 4. Pore size distribution of untreated HNT and silanised HNT (O-HNT) with OTES and caffeic acid-loaded HNT (CA- HNT).

Figure 5. FTIR spectrum of untreated HNT, silanised HNT with OTES (O-HNT).

Figure 6. FTIR spectrum of untreated HNT**,** caffeic acid-loaded HNT (CA-HNT).

Figure 7. SEM images of (a) unmodified HNT (b) modified HNT with triethoxy(octyl)silane (O-HNT) and (c) HNT loaded with caffeic acid (CA-HNT).

Figure 8. TGA of unmodified HNT and silanised HNT with OTES (O-HNT) and caffeic acid loaded HNT (CA-HNT).

Figure 9. TGA of unmodified HNT and silanised HNT with OTES (O-HNT) and caffeic acid loaded HNT (CA-HNT).

Tables Captions

Table 1. Chemical composition of HNT and treated HNT as obtained by XRF analysis.

Table 2. BET surface area and total pore volume of HNT, treated HNT with OTES and caffeic acid.

https://doi.org/10.1180/clm.2025.10013 Published online by Cambridge University Press